GEOPHYSICAL RESEARCH LETTERS, VOL. 26, NO. 11, PAGES 1573-1576, JUNE 1, 1999

The source region of an interplanetary type II radio burst

S. D. Bale[1], M. J. Reiner[2,3], J.-L. Bougeret[4], M. L. Kaiser[2], S. Krucker[1], D. E. Larson[1], and R. P. Lin[1,5]

Abstract. We present the first observation of the source region of an interplanetary type II radio burst, using instruments on the Wind spacecraft. Type II radio emission tracks the motion of a CME-driven interplanetary (IP) shock which encounters the spacecraft. Upstream of the IP shock backstreaming electrons are observed, first antiparallel to the interplanetary magnetic field (IMF), and then later parallel as well. Langmuir waves are observed concomitant with the shock-accelerated electrons. The electron energy spectrum and Langmuir wave amplitudes are very similar to those observed in the terrestrial electron foreshock. From the connection times to the shock, we infer the existence and characteristic size of large scale structure on the shock front. The type II radio emission seems to be generated in a small bay upstream of the shock, and this may account for some splitting structure observed in the frequency spectrum of many type II bursts.

1. Introduction

Interplanetary type II radio bursts are associated with Coronal Mass Ejections (CMEs) that originate at the Sun and propagate into interplanetary space. A shock often forms ahead of the CME as it propagates outward and radio emission, at f_{pe} and/or $2f_{pe}$, is thought to be generated by shock-accelerated electrons near this shock front [*Cane et al.*, 1981]. Fast interplanetary shocks ($v > 500$ km/s) associated with CMEs are generally thought to be required for the generation of the type II emission [*Cane et al.*, 1987], although recent observations from the Wind spacecraft suggest that even relatively slow CME-driven shocks ($v \approx 500$ km/s) can generate interplanetary type II emissions [*Reiner et al.*, 1998a].

There are some unresolved points in the theory of type II radio emission. Type II bursts were found to consist of diffuse background emissions with sporadic intensifications [*Cane et al.*, 1982]. *Reiner et al.* [1998b] suggested that some sporadic type II emissions correspond to emissions at various sites along the shock front. There has been a long standing controversy as to whether the type II emissions are generated upstream or downstream of the CME-driven shock [*Lengyel-Frey*, 1992]. From analyses of the characteristics of the type II frequency drift rates, *Reiner et al.* [1997a, 1998a,b] recently concluded that interplanetary type II radio emissions must be generated in the upstream region of the CME-driven shock. However, in spite of years of observational work, the electron beam in the radio source region of an interplanetary type II has never been observed *in situ*.

In this letter, we present the first direct observation of the source region of a type II radio burst. Velocity-dispersed electron beams are detected in the region upstream of an interplanetary shock. The simultaneous detection of Langmuir waves confirms that this is a source region of type II radio emission. Large scale shock structure is also inferred from these observations. These observations indicate that the type II radio emissions are generated in "bays" along the shock front; this could account for the fine frequency structure observed in some type II bursts.

2. Observations and analysis

At 22:09:11 UT on August 24, 1998, an X1.0 class flare was observed by the GOES-10 soft x-ray flux monitor and as an Hα flare at N35 E09 [Solar Geophysical Data, 1998]. Figure 1 shows a radio dynamic spectrum from the WAVES instruments on Wind [*Bougeret et al.*, 1995] (top panel) and GOES-10 x-ray flux data (bottom panel). An intense type III burst accompanies the flare x-ray flux. Intense, remotely observed type II emission is observed between 200-300 kHz early (between 02:00-04:00 UT) on August 25, 1998 at 0.16 AU from the Sun and then becomes weaker. The slowly frequency-drifting emission reintensifies early on August 26, 1998, and finally a CME-driven IP shock is observed *in situ* at 06:40 UT on August 26. Although the SOHO spacecraft was unavailable to confirm the CME, the observed IP shock was followed by a magnetic cloud-like structure usually associated with CME-driven shocks. The total transit time of the shock, from the peak of the x-ray flux to arrival at the spacecraft is about 32 hours. Type II radio emission is generated by the plasma emis-

[1]Space Sciences Laboratory, University of California, Berkeley
[2]NASA Goddard Space Flight Center, Greenbelt
[3]Also at Hughes STX, Lanham MD
[4]DESPA, Observatoire de Paris, Meudon
[5]Department of Physics, University of California, Berkeley

Paper number 1999GL900293.
0094-8276/99/1999GL900293$05.00

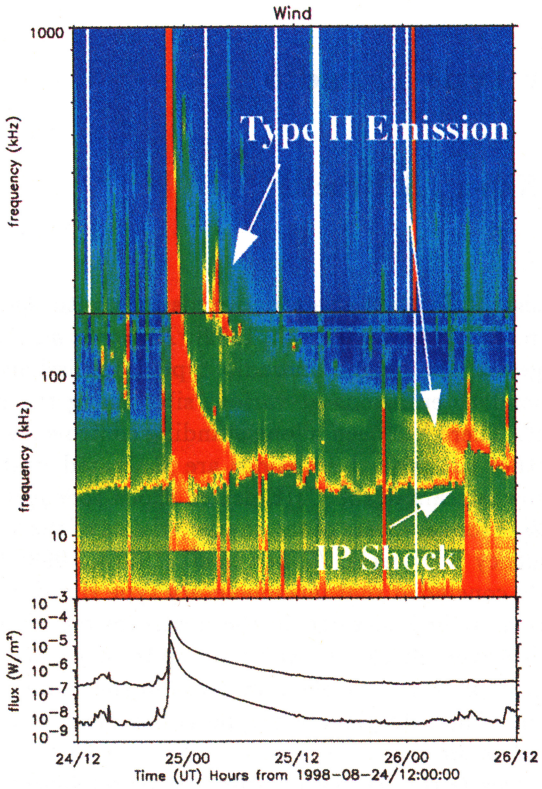

Figure 1. Radio wave and x-ray data for August 24-26, 1998. The top panel shows a dynamic spectrum from the WAVES experiment on Wind; the bottom panel is GOES-10 soft x-ray flux data. A flare at 22:09:11 UT on August 24, 1998 is evidenced by the abrupt onset of soft x-ray flux and the intense type III burst. The type II burst can be seen as the slowly frequency-drifting feature in the dynamic spectrum; the radio emission drifts down to meet an interplanetary shock at 06:40:24 UT on August 26, 1998. The upper trace of x-ray flux is flux in the band 1-8 Å and the lower trace is 0.5-4 Å.

sion process and so, occurs at either f_{pe} or $2f_{pe}$. Since the plasma density falls off as roughly $1/r^2$ in the solar wind, the plasma frequency goes as $1/r$, hence the observed frequency drift. The frequency drift rate of this burst is estimated to be 2.1 10^{-7} kHz^{-1} s^{-1}. The drift rate is the slope of the emission feature as plotted in $1/f$ vs. time and is linearly proportional to the speed of the IP shock.

Figure 2 shows *in situ* data from the WAVES, Three-Dimensional Plasma (3DP) [*Lin et al.*, 1995], and Magnetic Fields Investigation (MFI) [*Lepping et al.*, 1995] instruments on the Wind spacecraft near the time of the shock arrival. Panel (a) is a dynamic spectrum (in the range 4-256 kHz) from the Thermal Noise Receiver (TNR) component of WAVES showing Langmuir waves at f_{pe} beginning at 06:38:40 UT. Panel (b) is the TNR power at f_{pe} in units of $\mu V^2/Hz$. Panel (c) shows the measurement time and peak amplitude of electric field waveform events sampled by the WAVES Time Domain Sampler (TDS). The next three panels ((d), (e), and (f)) are electron flux parallel, perpendicular, and anti-parallel to the local interplanetary magnetic field (IMF) respectively, as measured by the low geometric factor electron electrostatic analyzer (EESA-L) instrument on 3DP, operating in burst mode. The EESA-L data is at 3 second time resolution and shows energies from 16-1140 eV. Panel (g) shows the solar wind proton density measured by the ion electrostatic analyzer (PESA-L) and the bottom panel (h) gives the magnitude of the IMF as measured by the MFI instrument.

The proton density and IMF magnitude show the arrival of the IP shock at 06:40:24 UT on August 26, 1998

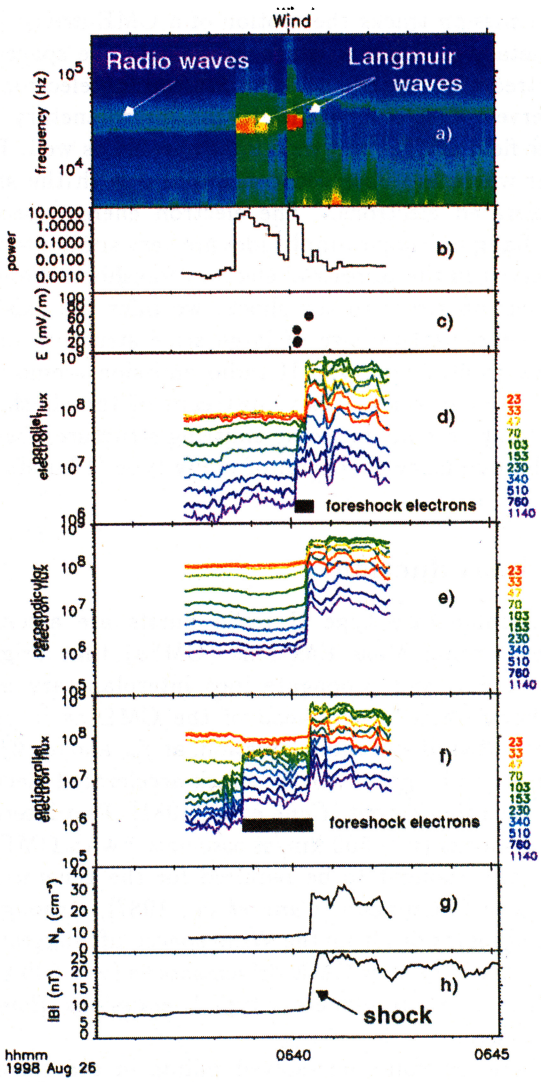

Figure 2. *In situ* particle and fields data from the WAVES, 3DP, and MFI instruments on the Wind spacecraft. Panels (g) and (h) show the density and magnetic field jump associated with the IP shock (at arrow in lower panel). The electron flux measurements (panels (f)-(d)) show the existence of a foreshock region upstream of the IP shock. Electrons in panel (d) are streaming away from the shock, parallel to the IMF; backstreaming electron in panel (f) are traveling anti-parallel to the IMF. Intense Langmuir waves are observed by the WAVES instrument (panels (a)-(c)) in the foreshock region. The units of electric field power (panel (b)) are $\mu V^2/Hz$; units of electron energy flux are $eV/sec/cm^2/ster/eV$.

at Wind, 120 R_e upstream of Earth. The ratio of upstream (unshocked) to downstream (shocked) IMF and proton density are $B_{down}/B_{up} \approx 3.3$ and $n_{down}/n_{up} \approx 3.7$. Assuming that the shock left the Sun at the time of the peak of the x-ray flux (22:09:11 UT, August 24, 1998), we estimate the average shock speed to be $v_{shock} \approx 1300$ km/s. The upstream solar wind speed is approximately 485 km/s, hence the average shock speed in the solar wind frame is approximately 815 km/s. A minimum variance analysis on the shock front gives a normal direction of $\hat{n} \approx (-0.93, -0.09, 0.36)$ in geocentric solar ecliptic (GSE) coordinates. The maximum to minimum eigenvalue ratio of the minimum variance calculation was 309, indicating an excellent result.

The average direction of the upstream IMF is $\hat{B} \approx (-0.13, 0.97, 0.02)$, again in GSE coordinates and averaged for three minutes upstream of the shock. Hence, the shock is quasi-perpendicular with $\Theta_{bn} = \cos^{-1}(\hat{B} \cdot \hat{n}) \approx 86°$, which seems reasonable due to the very discrete shock structure and lack of the large-scale upstream turbulence usually associated with quasi-parallel shocks. The IMF is very steady just upstream of the shock, with no variations in direction greater than 10° in the four minutes before the shock arrival. Using upstream sound and Alfvén speeds, and the average shock speed, we estimate the fast Mach number to be $M_f \approx 10$, while the Alfvén Mach number is $M_a \approx 13$, indicating a strong shock.

The electron flux data (panels d-f) show the presence of shock-accelerated electrons upstream of the IP shock. Panel (e) shows the flux perpendicular to the IMF and is steady upstream from the shock, showing large enhancement at and beyond the shock front. This shows the usual electron heating associated with strong MHD shocks. Panel (f) is electron flux in the $-\hat{B}$ direction and shows enhancements starting at around 06:38:15 UT. There is an abrupt increase in flux above roughly 70 eV at 06:38:40 UT, concurrent with the onset of the Langmuir waves. The flux remains fairly steady until just before the arrival of the IP shock, at which time the minimum energy of enhanced flux increases.

Electron flux parallel to $\hat{B}$ increases abruptly at 06:40:05 UT, approximately 20 seconds before the arrival of the shock. These electron flux enhancements are evidence of magnetic connection to the IP shock in the opposite direction. It should be noted that after 06:40:05 UT electrons are observed streaming in both directions, indicating that the IMF is connected to the shock at both ends.

Panel (a) shows the occurrence of intense plasma waves near the local plasma frequency f_{pe}; these enhancements are strongest just after magnetic connection in the antiparallel and parallel directions and decay closer to the shock (panel (b)). The most intense Langmuir waves during this type II event occur during the interval of counterstreaming, shock-accelerated electrons, after 06:40:05 UT. The TDS instrument (panel (c)) triggered on intense Langmuir waves at near 06:40:10 UT, during the interval of both enhanced parallel and antiparallel electron flux; the peak amplitude of these Langmuir waves is between 15 - 40 mV/m. A TDS event at 06:40:27 UT on the shock ramp shows an intense, spiky electrostatic waveform similar to those observed at Earth's bow shock [*Bale et al.*, 1998]; this event is more intense than the Langmuir wave events.

Taken together, the *in situ* data give concrete evidence of a foreshock region upstream of the IP shock. This region is marked by shock-accelerated electrons streaming away from the shock on connected IMF lines and would therefore be expected to form velocity-dispersed electron beams near the edge of the foreshock region [e. g. *Filbert and Kellogg*, 1979]. The terrestrial foreshock is also characterized by intense radio emission at f_{pe} and $2f_{pe}$ and it is very likely that the microphysics of the radio emission process is identical here. From Figure 2, it can be seen that the cutoff electron beam energy is between 100-150 eV; this corresponds to $v_b/v_{th} \approx 2.5$-3.5 using the upstream electron thermal speed. This is a factor of three lower than is typical near the terrestrial electron foreshock edge.

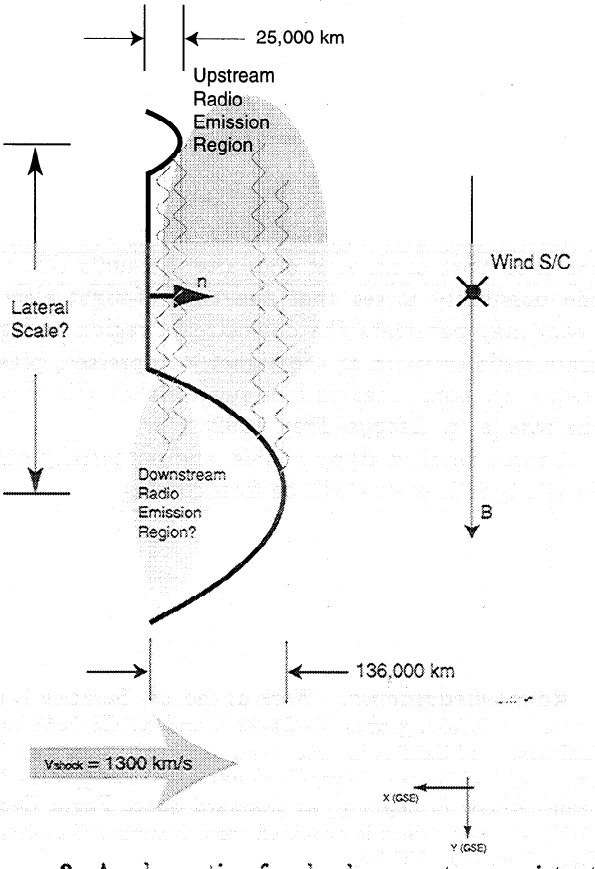

Figure 3. A schematic of a shock geometry consistent with our observations. Strong electron flux, in the $-\hat{B}$ direction, begins 105 seconds ahead of the shock, indicating magnetic connection to the shock surface 136,000 km upstream of where the spacecraft impacts the shock. Likewise, electron flux in the $+\hat{B}$ direction begins 19 seconds before impact, indicating shock structure extending 25,000 km upstream. Radio emission occurs near the upstream edge of each foreshock region, which may actually extend into the downstream region in the case of the later, $+\hat{B}$ connection.

3. Discussion

We present *in situ* observations of the radio source region of an interplanetary type II radio burst. This is the first such observation (known to us) and supports the proposition that type II radio waves are generated by the plasma emission process, as in the terrestrial electron foreshock and type III radio bursts. Furthermore, our observations suggest evidence of large-scale structure on the shock front. Figure 3 shows a schematic of possible shock structure consistent with our observations. Assuming a straight IMF line, in approximately the $+Y$ GSE direction and a shock normal in the $-X$ GSE direction, we can estimate the upper limit of the scale of this structure. The abrupt increase in electron flux in the $-\hat{B}$ direction at 06:38:40 UT corresponds to magnetic connection approximately 137,000 km (or 21 R_e) upstream of the shock. The increased flux parallel to B at 06:40:05 UT occurs at 26,000 km (4 R_e) upstream. The protruding surfaces of the shock connect magnetically before the shock arrives at the spacecraft. If the instantaneous shock speed is less than the average speed, the actual scale size of the structures will be smaller. Such shock structure might be caused by Alfvén speed inhomogenieties in the solar wind, which let some regions of the shock run ahead of others.

Radio emission will originate from the upstream edges of the observed foreshock regions, as in the terrestrial electron foreshock [*Filbert and Kellogg*, 1979; *Reiner et al.*, 1997b]. However, if the field line connects to the shock on both ends, as it does after 06:40:05 UT, then the possibility arises that the time-of-flight electron beam may penetrate the downstream region and generate radio emission at the higher, compressed, plasma frequency. Some observations suggest that this may be the case [e. g. *Lengyel-Frey*, 1992].

A more detailed study of this, and potentially other, *in situ* type II events will be forthcoming.

Acknowledgments. Work at the UC Berkeley is supported by NASA grants NAG5-2815 and NAG5-7961 to the University of California. MJR is supported in part by NSF grant ATM-9713422. Wind/MFI data is courtesy of the MFI team (PI: R. P. Lepping) at Goddard Space Flight Center. GOES-10 x-ray data is obtained from National Geophysical Data Center at NOAA.

References

Bale, S. D., P. J. Kellogg, D. E. Larson, R. P. Lin, K. Goetz, and R. P. Lepping, Bipolar electrostatic structures in the shock transition region: evidence of electron phase space holes, Geophys. Res. Lett., *25*, 2929, 1998.

Bougeret, J.-L., et al, WAVES: The radio and plasma wave investigation on the WIND spacecraft, *Space Science Rev.*, *71*, 231, 1995.

Cane, H. V., R. G. Stone, J. Fainberg, R. T. Stewart, J.-L. Steinberg, and S. Hoang, Radio evidence for shock acceleration of electrons in the solar corona, Geophys. Res. Lett., *12*, 1285, 1981.

Cane, H. V, R. G. Stone, J. Fainberg, J.L. Steinberg, and S. Hoang, Type II solar radio events observed in the interplanetary medium, *Solar Phys.*, *78*, 187, 1982.

Cane, H. V., N. R. Sheeley, Jr., and R. A. Howard, Energetic interplanetary shocks, radio emission, and coronal mass ejections, J. Geophys. Res., *92*, 9869, 1987.

Filbert, P. C., and P. J. Kellogg, Electrostatic noise at the plasma frequency beyond the Earth's bow shock, J. Geophys. Res., *84*, 1369, 1979.

Lengyel-Frey, D., Location of the radio emitting regions of interplanetary shocks, J. Geophys. Res., *97*, 1609, 1992.

Lepping, R. P., et al, The WIND magnetic field investigation, *Space Science Rev.*, *71*, 207, 1995.

Lin, R. P., et al, A three-dimensional plasma and energetic particle investigation for the WIND spacecraft, *Space Science Rev.*, *71*, 125, 1995.

Reiner, M. J., M. L. Kaiser, J. Fainberg, J.-L. Bougeret, R. G. Stone, Remote radio tracking of interplanetary CMEs, Proc. 31st ESLAB Symp., 'Correlated Phenomena at the Sun, in the Heliosphere and in Geospace', ESTEC, Noordwijk, The Netherlands, 183-188, 1997a.

Reiner, M. J., Y. Kasaba, M. L. Kaiser, H. Matsumoto, I. Nagano, and J.-L. Bougeret, Terrestrial $2f_{pe}$ radio source location determined from WIND/ Geotail triangulation, Geophys. Res. Lett., *24*, 919, 1997b.

Reiner, M. J., M. L. Kaiser, J. Fainberg, and R. G. Stone, A new method for studying remote type II radio emissions from coronal mass ejection-drive shocks, J. Geophys. Res., *103*, 29,651, 1998a.

Reiner, M. J., M. L. Kaiser, J. Fainberg, J.-L. Bougeret and R. G. Stone, On the origin of radio emissions associated with the January 6-11, 1997, CME, Geophys. Res. Lett., *25*, 2493, 1998b.

S. D. Bale, S. Krucker, D. E. Larson, and R. P. Lin, Space Sciences Laboratory, University of California, Berkeley, CA, 94720-7450 USA (email: bale@ssl.berkeley.edu)

J.-L. Bougeret, DESPA, Observatoire de Paris, Meudon 97005 FRANCE

M. L. Kaiser and M. J. Reiner, Laboratory for Extraterrestrial Physics, Goddard Space Flight Center, Greenbelt, MD 20771 USA

(Received March 3, 1999; revised April 5, 1999; accepted April 12, 1999.)